

Accounting for secondary inner filter effect in fluorescence spectra from solid samples

Tuhin Khan^{1,2}, Kalyani Bhagabani^{3,†},
Preeti Kumari^{4,†} and Anindya Datta^{1,*}

¹Department of Chemistry, Indian Institute of Technology Bombay, Powai, Mumbai 400 076, India

²Current address: Department of Applied Chemistry, Shri Govindram Seksaria Institute of Technology and Science, Indore 452 003, India

³School of Chemical Sciences, National Institute of Science Education and Research Bhubaneswar, Jatni 752 050, India

⁴Department of Chemistry, National Institute of Technology Calicut, Kozhikode 673 601, India

Fluorescence experiments at high fluorophore concentrations or in solid state have biological relevance and application potential in devices. Inner filter effect, arising from reabsorption of emitted photons, is the simplest of several factors that complicate the emission in these systems. This effect is prominent, especially for systems with small Stokes shift between absorption and emission. Solid state ‘dilution’ of a fluorophore with an optically transparent, non-interfering substance can significantly minimize this effect. This has been shown in the present study, using salophen as a fluorophore and NaCl as the dilutant. The general applicability of this method is tested with three more fluorophores.

Keywords: Aggregation-induced emission, inner filter effect, fluorescence spectroscopy, solid-state emitters.

IN view of the increasing interest in solid-state emitters, with application in optoelectronic devices, experiments involving fluorescence from solids are the order of the day^{1,2}. The biggest challenge in this endeavour is aggregation-caused quenching (ACQ) in solid state³. Suppression of ACQ and promotion of aggregation-induced emission (AIE) by manipulation of the chemical structure has been the subject of active research^{4,5}. In this context, it is important to recognize that the highly sensitive nature of fluorescence makes it susceptible to certain pitfalls; inner filter effect is one such example^{6,7}. It can be classified into primary and secondary effects. Primary inner filter effect involves significant absorption of excitation light by the front surface of the emitter and consequent decrease in the amount of excitation light that reaches the centre of the sample. This leads to a significant decrease in emission intensity and quantum yield. Fluorescence lifetimes are not affected, as the decrease in emission intensity is essentially due to a decrease in the amount of excitation light. There are several reports on

correction for primary inner filter effect in concentrated solutions^{8–10}.

Secondary inner filter effect is observed when there is a strong overlap between absorption and emission spectra, leading to the possibility of reabsorption of emitted light by another molecule in close vicinity. In this case, self-absorption of the blue end of emission results in distortion of the emission spectrum^{11–14}. In extreme situations, a progressive red shift (bathochromic shift) in emission maximum is observed with increase in concentration⁷. Generally, this problem is circumvented in solutions by keeping the absorbance low and modifying the cuvette dimensions^{6,11}. Fluorescence from solid-state emitters can be seriously corrupted by inner filter effect, and this poses a major problem in their quantitative analysis¹⁵. Distortion of the spectrum is more serious in crystalline solid emitters, in which intermolecular distances are small and path lengths are large due to crystal thickness. These issues need to be addressed while designing an experiment on solid emitters, both in amorphous and crystalline states, as a red shift in emission spectra is often reported for AIE-active molecules in their aggregated state^{16–20}. Secondary inner filter effect is manifested not only in decreased fluorescence quantum yield, but also in slower fluorescence decay. Both quantum yield and lifetime are affected by the extent of reabsorption of emitted light, which in turn is dependent on spectral overlap and sample concentration. The modulated fluorescence quantum yield (ϕ'_f) and lifetime (τ') are expressed using the equations²¹

$$\phi'_f = \frac{\phi_f(1-a)}{1-a \cdot \phi_f}, \quad (1)$$

$$\tau' = \frac{\tau}{1-a \cdot \phi_f}, \quad (2)$$

where a is the probability of reabsorption of emitted light by the sample. This term can be expressed as

$$a \cdot \phi_f = \int F(\bar{v}) \{1 - 10^{-\varepsilon(\bar{v})cx}\} d\bar{v}. \quad (3)$$

Here $F(\bar{v})$ and $\varepsilon(\bar{v})$ are fluorescence intensity and absorption coefficient respectively, c the concentration and x is the thickness of the sample from which the fluorescence travels^{21,22}. Birks and co-workers observed a dramatic decrease in secondary inner filter effect with decrease in crystal size and mixing the sample with another solid substance. For example, the fluorophore anthracene was diluted by mixing with naphthalene in their experiment²³. Here, we describe easy steps to detect and minimize secondary inner filter effect in a solid-state emitter by simply mixing it with varying amounts of NaCl. The experiment has been formulated using salophen

*For correspondence. (e-mail: anindya@chem.iitb.ac.in)

†Equally contributed.

(*N,N'*-bis-(salicylidene)-*o*-phenylenediamine), a Schiff base which is weakly fluorescent in solutions, but strongly fluorescent in solid state^{24,25}. Thus, it is an ideal candidate for aggregation-induced enhancement of emission and can be used as a solid-state emitter.

All chemicals were used as received. Salophen was synthesized in a one-step reaction, under ambient conditions. An ethanolic solution of *o*-phenylenediamine (500 mg) and salicylaldehyde (1 ml) in 1 : 2 mole ratio yielded orange precipitate in 10–15 min with high yield. The precipitate was washed with cold ethanol and diethyl ether. For fluorescence study, the sample was crystallized from hot saturated solution in ethanol. Fine needle-like crystals were formed within a few hours and they were washed with diethyl ether²⁴.

The spectra were recorded using a spectrometer (Varian Cary Eclipse) with an excitation wavelength (λ_{ex}) of 360 nm, keeping 5 nm fixed excitation and emission

bandpass. In view of the high concentration, it was not possible to use standard 1 cm cuvettes. Instead, a rectangular thin cuvette of 2 mm path length was used (Figure 1 *b*). Alternatively, the sample was packed between two quartz slides which were taped together (Figure 1 *b*). In experiments with solid emitters, the usual practice is to place the sample at the centre of the cuvette holder, at an optimum angle, so as to maximize the ratio of fluorescence intensity (at emission maximum) to scattering intensity (at $\lambda_{\text{ex}} + 10$ nm). The angle is determined by trial and error. In the present experiment, a normal angle of incidence was used, in order to minimize the interference from scattered light and achieve reproducibility of the position of the sample. The sample was placed behind the central position, indicated by a dashed line in Figure 1 *c*. This position is important, as it ensures collection of emitted light exclusively from the front surface and thus minimizes secondary inner filter effect^{15,26,27}. In this condition, the emission of salophen is observed at 560 nm (Figure 2 *a*).

Salophen crystals were crushed to powder for measurement in pure solid form, so as to decrease the effective path length and hence minimize secondary inner filter effect. In some cases, this process can lead to a change in spectral shape. Such an observation would confirm that secondary inner filter effect is operative²³. The matrix for solid-state dilution of the sample was chosen based on purity (no fluorescence), optical transparency and non-interacting nature. NaCl satisfies these requirements perfectly well. To make mixing of the sample and NaCl more effective and homogenous, the salt was crushed to powder. A rectangular cuvette was used for experiments performed on diluted samples. This is necessary because NaCl, being a hard crystalline solid, cannot be packed effectively between two quartz slides. A change in spectral shape of salophen emission was observed upon progressive dilution, accompanied by the appearance of an emission maximum at 530 nm. The emission spectrum was found to be broad at intermediate values of dilution (1% weight of salophen), with contribution from both the emission maxima. At a dilution of 0.05% of salophen prominent peak at 530 nm was observed whereas the 560 nm peak was reduced to shoulder (Figure 2 and [Supplementary Figure 1](#)). With dilution the fluorescence decays were found to be marginally faster ([Supplementary Figure 2](#)). Use of KCl in place of NaCl as dilutant gave similar results. The occurrence of secondary inner filter effect was confirmed by monitoring fluorescence from the front surface (reflection mode) and back surface (transmission mode). In the presence of secondary inner filter effect emission monitored from the back surface (transmission mode) was expected to be distorted due to reabsorption. At an intermediate dilution (~2% weight of salophen), the spectra corresponding to reflection mode and transmission mode were found to be significantly different (Figure 3 *a*). The emission monitored

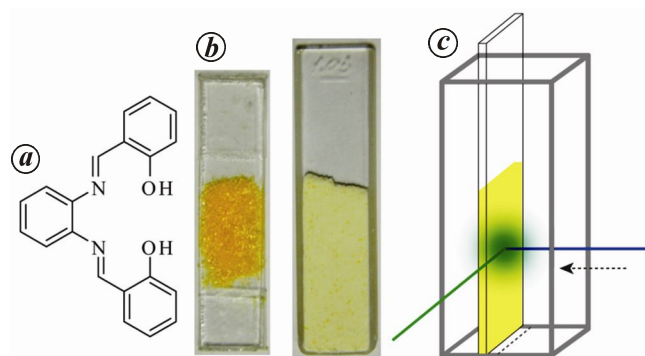


Figure 1. *a*, Chemical structure of salophen. *b*, (Left) Salophen crystals sandwiched between two quartz slides, (Right) Crushed salophen crystals diluted with NaCl. *c*, Orientation of the solid sample in cuvette holder of the fluorimeter. Blue line indicates the direction of excitation light and green line indicates the direction in which fluorescence from the sample is collected. The dotted line denotes the plane passing through the centre of the base and parallel to the side on which fluorescence is incident.

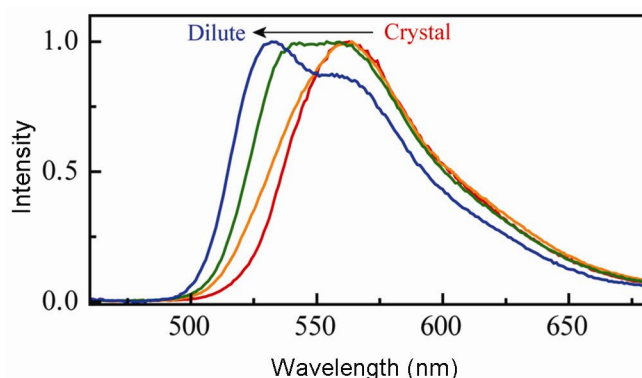


Figure 2. Peak normalized fluorescence spectra of salophen on dilution with NaCl. The most red-shifted spectrum (red) is for pure crystal and the most blue-shifted spectrum (blue) is for 0.05% (w/w) of salophen. A fluorescence spectrum of NaCl diluted salophen has been reported in our recent publication²⁵.

from the front surface was found to have a strong additional shoulder around 530 nm. The difference decreased with dilution and became superimposable when self-absorption was minimized to a great extent (Figure 3 *b* and [Supplementary Figure 3](#)). Minimization of secondary inner filter effect by dilution with NaCl was verified for other molecules exhibiting solid-state fluorescence. Transition metal complex ruthenium trisbipyridine ($[\text{Ru}(\text{bpy})_3]^{2+}$) in its pure solid form emits at 600 nm. When diluted with NaCl the spectrum becomes more structured with strong peak at 580 nm and a shoulder at 610 nm (Figure 4 *a*).

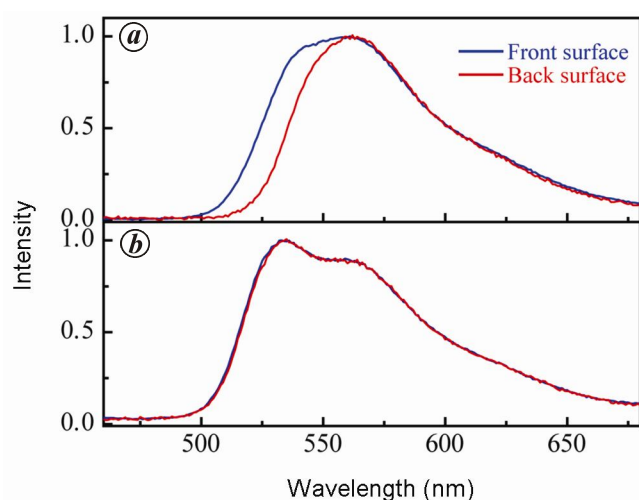


Figure 3. Variation of fluorescence spectra when monitored from the front surface (blue) and back surface (red) in (a) moderately diluted sample (~2%) and (b) significantly diluted sample (~0.05%).

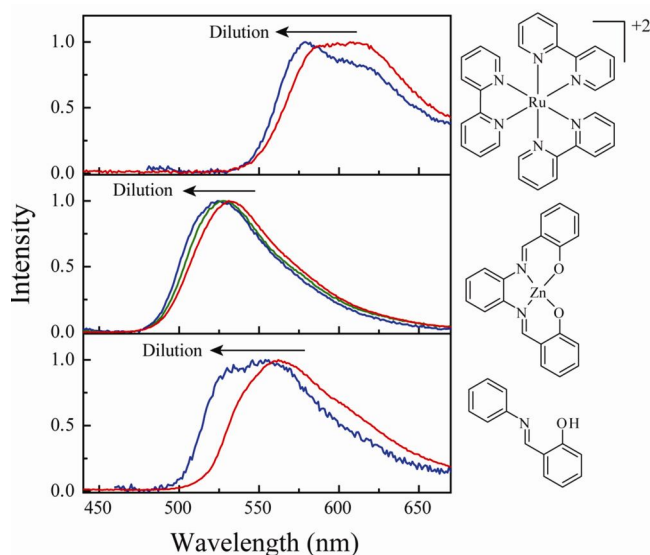


Figure 4. Chemical structure and the effect of dilution on ruthenium trisbipyridine (top), zinc complex of salophen (middle) and *N*-salicylideneaniline (bottom). Zinc complex of salophen is fibrous in nature. All samples are excited at 360 nm and the spectra are [0, 1] normalized for better comparison. In the diluted sample weak signal and strong scattering limit the spectral range.

This profile closely resembles its emission spectra at 77 K (ref. 28). Zinc complex of salophen has red-shifted emission in solid state with respect to solution phase²⁵. When it is diluted with NaCl progressive blue shift (hypsochromic shift) in fluorescence maximum is observed (Figure 4 *b*). Schiff base *N*-salicylideneaniline has a broad emission peaking at 560 nm. When it is mixed with NaCl, the spectra get broadened with the appearance of a distinct shoulder at 530 nm, similar to salophen (Figure 4 *c*).

In conclusion, we have studied secondary inner filter effect in solid state, which can otherwise skew spectral profiles. The effect can be detected and minimized through dilution with simple salts such as NaCl. All four samples studied here underwent blue shift in emission upon dilution with NaCl. This easy and short experiment may be useful in highlighting pitfalls in the interpretation of red shift of fluorescence spectra from solution to solid state, especially for fluorophores with small Stokes shift. The simple act of solid-state dilution can address the issue of secondary inner filter effect and help in the interpretation of spectra in experiments involving AIE.

1. Padalkar, V. S. and Seki, S., Excited-state intramolecular proton-transfer (ESIPT)-inspired solid state emitters. *Chem. Soc. Rev.*, 2016, **45**, 169–202.
2. Kupcewicz, B. and Malecka, M., Role of Crystal packing and weak intermolecular interactions in the solid state fluorescence of *N*-methylpyrazoline derivatives. *Cryst. Growth Des.*, 2015, **15**, 3893–3904.
3. Das, U. K. and Dastidar, P., Aggregation enhanced emission (AEE) in organic salt: a structure–property correlation based on single crystal studies. *J. Chem. Sci.*, 2014, **126**, 1357–1362.
4. Mei, J., Leung, N. L. C., Kwok, R. T. K., Lam, J. W. Y. and Tang, B. Z., Aggregation-induced emission: together we shine, united we soar! *Chem. Rev.*, 2015, **115**, 11718–11940.
5. Hong, Y., Lam, J. W. Y. and Tang, B. Z., Aggregation-induced emission. *Chem. Soc. Rev.*, 2011, **40**, 5361–5388.
6. Kvittingen, E. V., Kvittingen, L., Melø, T. B., Sjørnsnes, B. J. and Verley, R., Demonstrating basic properties of spectroscopy using a self-constructed combined fluorimeter and UV-photometer. *J. Chem. Educ.*, 2017, **94**, 1486–1491.
7. Lakowicz, J. R., *Principles of Fluorescence Spectroscopy*, Springer, New York, USA, 3rd edn., 2006.
8. Kubista, M., Sj back, R., Eriksson, S. and Albinsson, B., Experimental correction for the inner-filter effect in fluorescence spectra. *Analyst*, 1994, **119**, 417–419.
9. Fonin, A. V., Sulatskaya, A. I., Kuznetsova, I. M., Turoverov, K. K. and Saito, T., Fluorescence of dyes in solutions with high absorbance. Inner filter effect correction. *PLoS One*, 2014, **9**, e103878.
10. Nettles, C. B., Hu, J. and Zhang, D., Using water Raman intensities to determine the effective excitation and emission path lengths of fluorophotometers for correcting fluorescence inner filter effect. *Anal. Chem.*, 2015, **87**, 4917–4924.
11. Fery-Forgues, S. and Lavabre, D., Are fluorescence quantum yields so tricky to measure? A demonstration using familiar stationery products. *J. Chem. Educ.*, 1999, **76**, 1260.
12. Riesz, J., Gilmore, J. and Meredith, P., Quantitative photoluminescence of broad band absorbing melanins: a procedure to correct for inner filter and re-absorption effects. *Spectrochim. Acta Part A*, 2005, **61**, 2153–2160.

13. Territo, P. R., Heil, J., Bose, S., Evans, F. J. and Balaban, R. S., Fluorescence absorbance inner-filter decomposition: the role of emission shape on estimates of free Ca^{2+} using Rhod-2. *Appl. Spectrosc.*, 2007, **61**, 138–147.
14. Iasilli, G. *et al.*, Aggregation-induced emission of tetraphenylethylene in styrene-based polymers. *Macromol. Chem. Phys.*, 2014, **215**, 499–506.
15. Lagorio, M. G. and San Romn, E., How does light scattering affect luminescence? Fluorescence spectra and quantum yields in the solid phase. *J. Chem. Educ.*, 2002, **79**, 1362–1367.
16. Maar, R. R. and Gilroy, J. B., Aggregation-induced emission enhancement in boron difluoride complexes of 3-cyanoformazanates. *J. Mater. Chem. C*, 2016, **4**, 6478–6482.
17. Singh, R. S. *et al.*, Morphological tuning via structural modulations in AIE luminogens with the minimum number of possible variables and their use in live cell imaging. *Chem. Commun.*, 2015, **51**, 9125–9128.
18. Srivastava, A. K. *et al.*, Pyridyl substituted 4-(1,3-dioxo-1H,3H-benzo[de]isoquinolin-2-ylmethyl)-benzamides with aggregation enhanced emission and multi-stimuli-responsive properties. *J. Lumin.*, 2017, **182**, 274–282.
19. Feng, Q., Wang, M., Dong, B., Xu, C., Zhao, J. and Zhang, H., Tuning solid-state fluorescence of pyrene derivatives via a cocrystal strategy. *CrystEngComm*, 2013, **15**, 3623.
20. Khan, T. and Datta, A., Enhanced fluorescence with nanosecond dynamics in the solid state of metal ion complexes of alkoxy salophens. *Phys. Chem. Chem. Phys.*, 2017, **19**, 30120–30127.
21. Birks, J. B., *Photophysics of Aromatic Molecules*, Wiley-Interscience, London, 1970, 2nd edn.
22. Prunty, S. L., The effect of absorption on the quantum efficiency and decay-time in organic scintillators. *Nucl. Instrum. Methods Phys. Res., Sect.*, 1986, **245**, 563–565.
23. Birks, J. B. and Wright, G. T., Fluorescence spectra of organic crystals. *Proc. Phys. Soc. Sect. B*, 1954, **67**, 657–663.
24. Khan, T., Vaidya, S., Mhatre, D. S. and Datta, A., The prospect of salophen in fluorescence lifetime sensing of Al^{3+} . *J. Phys. Chem. B*, 2016, **120**, 10319–10326.
25. Khan, T. and Datta, A., Impact of molecular arrangement and torsional motion on the fluorescence of salophen and its metal complexes. *J. Phys. Chem. C*, 2017, **121**, 2410–2417.
26. Leese, R. A. and Wehry, E. L., Corrections for inner-filter effects in fluorescence quenching measurements via right-angle and front-surface illumination. *Anal. Chem.*, 1978, **50**, 1193–1197.
27. Ventura, B. *et al.*, Luminescence Properties of 1,8-naphthalimide derivatives in solution, in their crystals and in co-crystals: toward room-temperature phosphorescence from organic materials. *J. Phys. Chem. C*, 2014, **118**, 18646–18658.
28. Kirgan, R. A., Witek, P. A., Moore, C. and Rillema, D. P., Physical, photophysical and structural properties of ruthenium(ii) complexes containing a tetradentate bipyridine ligand. *Dalton Trans.*, 2008, 3189.

ACKNOWLEDGEMENTS. T.K. thanks CSIR, New Delhi and Industrial Research and Consultancy Centre, Indian Institute of Technology Bombay for research fellowship; K.B. thanks Department of Science and Technology for an INSPIRE fellowship and A.D. thanks National Centre for Photovoltaic Research and Education, IIT Bombay for research funds.

Received 25 October 2017; revised accepted 7 February 2018

doi: 10.18520/cs/v114/i11/2353-2356

Asp72 of pro-peptide is an important pH sensor in the zymogen activation process of papain: a structural and mechanistic insight

Sumana Roy¹ and Sampa Biswas^{1,2,*}

¹Crystallography and Molecular Biology Division, Saha Institute of Nuclear Physics, 1/AF Bidhannagar, Kolkata 700 064, India

²Homi Bhabha National Institute, Anushakthinagar, Mumbai 400 094, India

The zymogen of papain contains a pro-peptide at the N-terminus of the catalytic domain. Pro-peptide contains residues which act as pH-sensors in zymogen activation cascade. To understand the influence of pro-peptide in the pH-induced zymogen activation process of the protease, we performed structural studies of the zymogen of papain at activation pH of 4.0. The X-ray structure of zymogen at acidic pH reveals that Asp72 of the pro-peptide, a highly conserved residue of the GXNFXD motif, plays an important role in pH-induced conformational changes in the pro-domain leading to the zymogen activation process. Far-UV circular dichroism spectrum of zymogen at pH 4.0 demonstrates loss of helical structure compared to that at pH 8.0. The structural observation is further corroborated by mutational studies, where D72A mutant is shown to undergo auto-activation at pH 5.0 compared to pH 4.0 for wild-type, though the general proteolytic activity of the D72A mutant remains similar to that of wild-type. Our findings indicate that the conserved Asp72 residue is an important pH sensor in the zymogen activation process and that the pro-peptide part can also be a useful target of protein engineering for altering the activation pH of a protease.

Keywords: Cysteine protease, pH regulation, protein engineering, pro-peptide, X-ray crystallography.

PAPAIN (EC 3.4.22.2), a cysteine protease from the tropical plant *Carica papaya*, has considerable commercial significance because of its wide uses in various industrial processes¹. It also has different medical applications like in gastric fermentation, gastritis, to assist protein digestion in chronic dyspepsia, preparation of tyrosine derivatives for the treatment of Parkinsonism, removal of necrotic tissue, preparation of tetanus vaccines, cleansing agents of skin, treatments of acne, etc.². Papain has been characterized extensively from the kinetic, molecular and structural point of view^{3,4}. It is the first proteolytic enzyme whose crystal structure was determined in 1968 (ref. 5). Papain, the archetype enzyme of papain-like cysteine proteases (clan C1A) shares a common fold with other members of the family having a molecular weight

*For correspondence. (e-mail: sampa.biswas@saha.ac.in)